Pattern Recognition, Vol. 24, No. 6, pp. 505–513, 1991
Printed in Great Britain

0031-3203/91 $3.00 + .00
Pergamon Press plc

SENSITIVITY ANALYSIS FOR MATCHING AND POSE COMPUTATION USING DIHEDRAL JUNCTIONS

S. M. BHANDARKAR*† and MINSOO SUK‡

*Department of Computer Science, 415 Graduate Studies Research Center, University of Georgia, Athens, GA 30602, U.S.A.; ‡Department of Electrical and Computer Engineering, 111 Link Hall, Syracuse University, Syracuse, NY 13244–1240, U.S.A.

(*Received* 27 *October* 1989; *in revised form* 3 *May* 1990; *received for publication* 29 *May* 1990)

Abstract—Recognition-via-localization is a popular approach in 3-D object recognition. This approach relies on the propagation of constraints that arise from the matches of local geometric features and could therefore be treated as a constraint satisfaction problem. Hough clustering, which verifies the consistency of local geometric constraints by determining the pose of the object in parameter space, is a popular technique owing to its conceptual simplicity and potential ease of parallelization. Our previous work has shown the usefulness of dihedral junctions for the recognition and localization of polyhedral objects and dihedral feature junctions for the recognition and localization of curved objects made up of piecewise combinations of conical, cylindrical and spherical surfaces. Experimental results from our previous work showed that the computed pose parameters are sensitive to the difference in the included angle between the scene and model dihedral junctions or the scene and model dihedral feature junctions. A formal analysis of the sensitivity of the computed pose to the difference in the included angle between the scene and model dihedral junctions or the scene and model dihedral feature junctions is presented in this paper. The results of the formal sensitivity analysis were found to be in conformity with the experimental results from our previous work and so the work presented in this paper could be treated as a sequel to our previous work. Based on the results of the sensitivity analysis, the rotation parameters were found to be more sensitive than the translation parameters which, in comparison, were far more robust. It is also shown how the introduction of redundancy in parameter space results in greater robustness in the computed pose. Although the analysis in this paper is based on the matching of dihedral junctions or dihedral feature junctions, the approach taken in the sensitivity analysis is general and can be applied to the matching based on other feature types.

Model-based vision Pose clustering Pose computation Sensitivity analysis

1. INTRODUCTION

Recognition-via-localization is a popular paradigm in 3-D object recognition. This approach relies on the propagation of constraints that arise from the matches of local geometric features and could therefore be treated as a constraint satisfaction problem. Hough clustering and searching the interpretation tree[6] are commonly used techniques for constraint propagation/constraint satisfaction in the recognition-via-localization approach to 3-D object recognition. Hough clustering, which verifies the consistency of local geometric constraints by determining the pose of the object in parameter space, is a popular technique owing to its conceptual simplicity and potential ease of parallelization. Each match of a scene feature with a model feature is used to compute a geometric transform which would place the geometric feature in registration with the scene feature. In 3-D space with six degrees of freedom this transform can be uniquely specified by six parameters—three translations one along each of the coordinate axes and three rotations one about each of the coordinate axes. Thus each geometric transform that is computed by matching a scene feature with a model feature can be represented by a point in six-dimensional Hough space or parameter space. Clustering or histogramming of points in Hough space is used to detect maxima or peaks which represent pose hypotheses.

In the application of Hough clustering to 3-D object recognition,[1–3] there exists a wide variety in the choice of features for matching and pose computation. The features chosen for recognition and localization should satisfy the following criteria:

(i) two non-parallel edges (which may be coplanar);

(ii) one edge and one face normal such that they are neither parallel nor perpendicular;

(iii) three face normals no two of which are parallel;

(iv) two parallel edges and one face normal which is not perpendicular to either of them;

(v) two face normals and one edge which is not perpendicular to either of the face normals.

These feature types are illustrated in Fig. 1.

† Author to whom correspondence should be addressed.

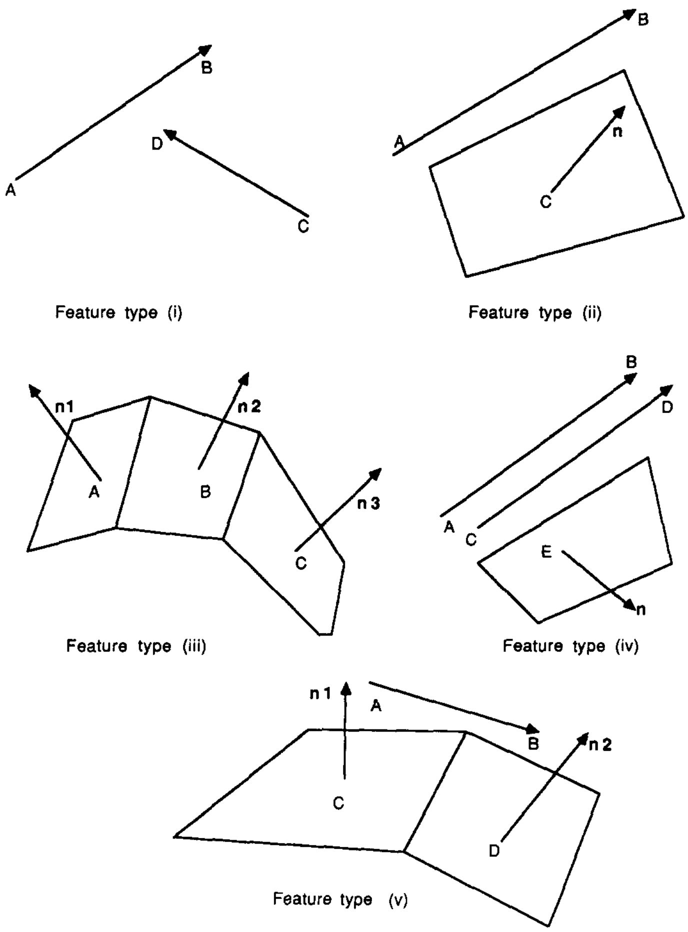

Fig. 1. Feature types of polyhedral object recognition.

In our previous work[4] we had developed a Hough clustering technique for the recognition and localization of polyhedral solids based on matching and pose computation using dihedral junctions. As shown in Fig. 2, dihedral junctions are junctions with a single vertex and two incident edges. Dihedral junctions are a subset of feature type (i). The results for the recognition and localization of polyhedral objects are extended to the recognition and localization of objects made up of piecewise combinations of conical, cylindrical and spherical surfaces.[5] Dihedral feature junctions are chosen as features for matching and localization. Examples of dihedral feature junctions are shown in Figs 3 and 4. Dihedral feature junctions are junctions formed from localization features for each of the surface types, i.e. conical, cylindrical, spherical and planar surface types.[7] The mathematical analysis underlying the matching and pose computation for both dihedral junctions and

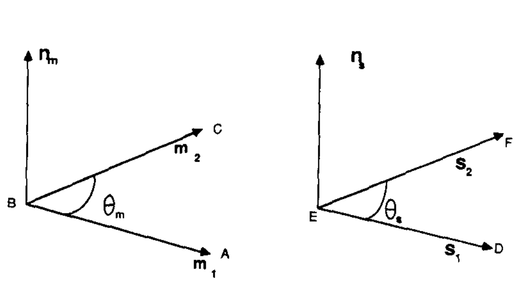

Fig. 2. Matching candidate model and scene dihedral junctions.

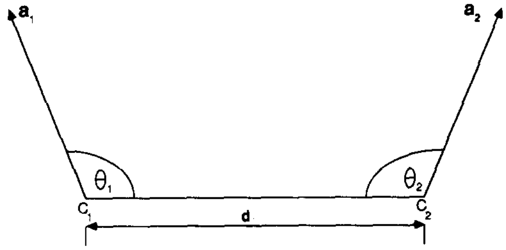

C_1 C_2 : apex of conical surface or centroid of cylindrical surface or centroid of planar surface.

a_1 a_2 : axis of conical or cylindrical surface or normal to the planar surface

Fig. 3. Type I: dihedral feature junction pair.

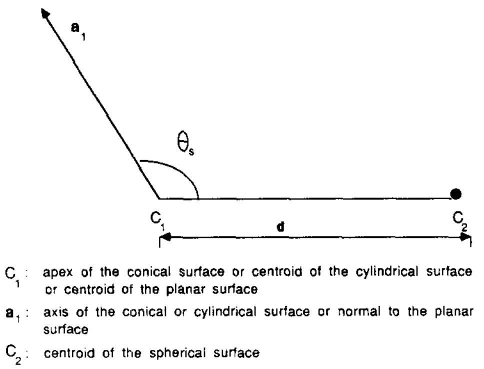

Fig. 4. Type II: dihedral feature junction.

dihedral feature junctions is identical, and hence only the matching and pose computation using dihedral junctions will be considered in this paper.

Owing to the errors introduced during the process of segmentation and feature extraction, the matching of scene features with model features is not exact. A certain amount of tolerance has to be incorporated during the process of matching a scene feature with a model feature. The tolerance introduced in the matching process is reflected as an error in the computed pose parameters. During the course of our experiments based on the matching and pose computations using dihedral junctions, the computed pose parameters were found to be sensitive to the difference in the included angles of the model dihedral junction (θ_m) and the scene dihedral junction (θ_s). The rotation parameters were found to be much more sensitive than the translation parameters which were more robust to differences in the included angle between the model and scene dihedral junctions. The objective of this paper is to present a formal analysis of sensitivity of the computed pose to the difference in the included angles of the model and scene dihedral junctions. The analysis substantiates experimental results cited in our previous work[4,5] and hence can be treated as a sequel to this work. Although the analysis is based on the matching of dihedral or dihedral feature junctions, the approach taken in the sensitivity analysis is general and can be applied to matching based on other feature types such as the ones shown in Fig. 1.

2. JUNCTION MATCHING AND POSE DETERMINATION

Figure 2 shows a model dihedral junction which is to be matched to a scene dihedral junction. With reference to Fig. 2, let $\mathbf{m}_1$ be the unit vector in the direction **BA** and let $\mathbf{m}_2$ be the unit vector in the direction **BC**. Similarly, let $\mathbf{s}_1$ be the unit vector in the direction **ED** and $\mathbf{s}_2$ be the unit vector in the direction **EF**. Let the homogeneous coordinates of B in the model coordinate system be $[x_0, y_0, z_0, 1]^T$ and let those of E in the scene coordinate system be $[u_0, v_0, w_0, 1]^T$. The goal is to find a transformation **T** such that

$$\mathbf{T}[x_0, y_0, z_0, 1]^T = [u_0, v_0, w_0, 1]^T. \tag{1}$$

T is determined in a stepwise manner as follows:

(1) Points B and E are translated to their respective origins. Let TRANS($-B$) and TRANS($-E$) denote the respective homogeneous transformation. This ensures that both junctions have their vertices translated to the origin.

(2) The vectors $\mathbf{m}_1$ and $\mathbf{m}_2$ are rotated about **k** through an angle θ so as to end up aligned with $\mathbf{s}_1$ and $\mathbf{s}_2$, respectively. **k** is determined by the requirement that it be perpendicular to both $\mathbf{m}_1 - \mathbf{s}_1$ and $\mathbf{m}_2 - \mathbf{s}_2$, or equivalently that the projections of $\mathbf{m}_1$ and $\mathbf{s}_1$ along **k** be equal and the projections of $\mathbf{m}_2$ and $\mathbf{s}_2$ along **k** be equal, i.e.

$$\mathbf{k}\cdot\mathbf{m}_1 = \mathbf{k}\cdot\mathbf{s}_1 \Rightarrow \mathbf{k}\cdot(\mathbf{m}_1 - \mathbf{s}_1) = 0 \tag{2}$$

$$\mathbf{k}\cdot\mathbf{m}_2 = \mathbf{k}\cdot\mathbf{s}_2 \Rightarrow \mathbf{k}\cdot(\mathbf{m}_2 - \mathbf{s}_2) = 0. \tag{3}$$

Thus

$$\mathbf{k} = \frac{(\mathbf{m}_1 - \mathbf{s}_1)\otimes(\mathbf{m}_2 - \mathbf{s}_2)}{|(\mathbf{m}_1 - \mathbf{s}_1)\otimes(\mathbf{m}_2 - \mathbf{s}_2)|} \tag{4}$$

where $\otimes$ denotes the vector cross product. From Fig. 5, we have

$$\overrightarrow{OA} = (\mathbf{m}_1\cdot\mathbf{k})\mathbf{k} = (\mathbf{s}_1\cdot\mathbf{k})\mathbf{k} \tag{5}$$

$$\overrightarrow{AC} = \mathbf{m}_1 - (\mathbf{m}_1\cdot\mathbf{k})\mathbf{k} \tag{6}$$

$$\overrightarrow{AC}\cdot\mathbf{k} = [\mathbf{m}_1 - (\mathbf{m}_1\cdot\mathbf{k})\mathbf{k}]\cdot\mathbf{k} = 0 \tag{7}$$

(since **k** is a unit vector as in (4)). Hence OAC is a right angle triangle with OC as the hypotenuse. Also,

$$|\overrightarrow{AC}| = |\overrightarrow{AB}| = \sqrt{1 - (\mathbf{m}_1\cdot\mathbf{k})(\mathbf{s}_1\cdot\mathbf{k})} \tag{8}$$

(since $\mathbf{m}_1$ is a unit vector). Therefore, θ is determined by

$$\cos\theta = \frac{\overrightarrow{AB}\cdot\overrightarrow{AC}}{|\overrightarrow{AB}||\overrightarrow{AC}|} = \frac{[\mathbf{m}_1 - (\mathbf{m}_1\cdot\mathbf{k})\mathbf{k}]\cdot[\mathbf{s}_1 - (\mathbf{s}_1\cdot\mathbf{k})\mathbf{k}]}{[1 - (\mathbf{m}_1\cdot\mathbf{k})(\mathbf{s}_1\cdot\mathbf{k})]} \tag{9}$$

$$= 1 - \frac{[1 - (\mathbf{m}_1\cdot\mathbf{s}_1)]}{[1 - (\mathbf{k}\cdot\mathbf{m}_1)(\mathbf{k}\cdot\mathbf{s}_1)]}. \tag{10}$$

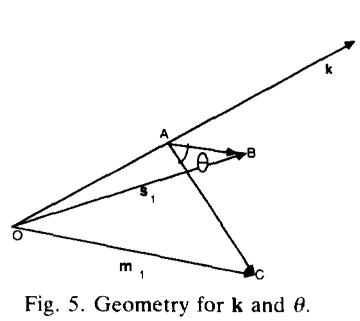

Fig. 5. Geometry for **k** and θ.

(3) The final transformation can thus be written as:

$$\mathrm{ROT}(k,\theta)\,\mathrm{TRANS}(-B)[x_0, y_0, z_0, 1]^T = \mathrm{TRANS}(-E)[u_0, v_0, w_0, 1]^T. \quad (11)$$

From (1) and (11)

$$\mathbf{T} = \mathrm{TRANS}^{-1}(-E)\mathrm{ROT}(k,\theta)\mathrm{TRANS}(-B). \quad (12)$$

The transformation **T** from the model coordinate system to the scene coordinate system could be thus written as:[8,9]

$$\mathbf{T} = \mathrm{ROT}(\mathbf{k},\theta)\mathrm{TRANS}(t_x, t_y, t_z) = \begin{bmatrix} r_{11} & r_{12} & r_{13} & 0 \\ r_{21} & r_{22} & r_{23} & 0 \\ r_{31} & r_{32} & r_{33} & 0 \\ 0 & 0 & 0 & 1 \end{bmatrix} \begin{bmatrix} 1 & 0 & 0 & t_x \\ 0 & 1 & 0 & t_y \\ 0 & 0 & 1 & t_z \\ 0 & 0 & 0 & 1 \end{bmatrix} \quad (13)$$

where

$$\begin{aligned} r_{11} &= k_x^2(1-\cos\theta)+\cos\theta \\ r_{12} &= k_xk_y(1-\cos\theta)-k_z\sin\theta \\ r_{13} &= k_xk_z(1-\cos\theta)+k_y\sin\theta \\ r_{21} &= k_xk_y(1-\cos\theta)+k_z\sin\theta \\ r_{22} &= k_y^2(1-\cos\theta)+\cos\theta \\ r_{23} &= k_yk_z(1-\cos\theta)-k_x\sin\theta \\ r_{31} &= k_xk_z(1-\cos\theta)-k_y\sin\theta \\ r_{32} &= k_yk_z(1-\cos\theta)+k_x\sin\theta \\ r_{33} &= k_z^2(1-\cos\theta)+\cos\theta \end{aligned} \quad (14)$$

and

$$\begin{aligned} t_x &= u_0 - r_{11}x_0 - r_{12}y_0 - r_{13}z_0 \\ t_y &= v_0 - r_{21}x_0 - r_{22}y_0 - r_{23}z_0 \\ t_z &= w_0 - r_{31}x_0 - r_{32}y_0 - r_{33}z_0. \end{aligned} \quad (15)$$

The axis of rotation **k** could be alternatively expressed by the pair (ξ, η) where

$$k_x = \cos\xi\sin\eta,\ k_y = \sin\xi\sin\eta,\ k_z = \cos\eta \quad (16)$$

where $-\pi < \eta < \pi$ and $0 < \xi < 2\pi$.

The transformation **T** is thus uniquely specified by the 6-tuple $(t_x, t_y, t_z, \xi, \eta, \theta)$.

3. SENSITIVITY ANALYSIS

In this section, sensitivity of the pose (i.e. rotation) parameters (ξ, η, θ) and translation parameters (t_x, t_y, t_z) to the difference in the included angles of the scene dihedral junction and the model dihedral junction is formally analysed.

As shown in Fig. 6, two dihedral junctions are said to match if $\theta_s = \theta_m$. In order to explore the case

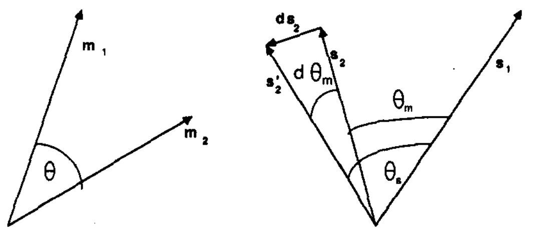

Fig. 6. Error in matching dihedral junctions.

where $\theta_m \neq \theta_s$ let $\theta_s = \theta_m + \mathrm{d}\theta_m$ then $\mathbf{s}_2' = \mathbf{s}_2 + \mathrm{d}\mathbf{s}_2$ where $|\mathbf{s}_2| = \mathrm{d}\theta_m$.

We explore three possible cases which arise in the matching of dihedral junctions.

Case 1.

$$\mathbf{m}_1 = \mathbf{s}_1 \Rightarrow \mathbf{k} = \mathbf{s}_1 = \mathbf{m}_1 \quad (17)$$

thus

$$\mathrm{d}\mathbf{k} = 0, \quad (18)$$

$$\mathbf{m}_1 \cdot \mathbf{m}_2 = \mathbf{k} \cdot \mathbf{m}_2 = \cos\theta_m \text{ and } \mathbf{s}_1 \cdot \mathbf{s}_2 = \mathbf{k} \cdot \mathbf{s}_2 = \cos\theta_m \quad (19)$$

since

$$\cos\theta = 1 - \frac{[1 - (\mathbf{m}_2 \cdot \mathbf{s}_2)]}{[1 - (\mathbf{k}\cdot\mathbf{m}_2)(\mathbf{k}\cdot\mathbf{s}_2)]} \quad (20)$$

$$\mathrm{d}(\cos\theta) = -\mathrm{d}\left[\frac{1 - (\mathbf{m}_2 \cdot \mathbf{s}_2)}{1 - (\mathbf{k}\cdot\mathbf{m}_2)(\mathbf{k}\cdot\mathbf{s}_2)}\right]. \quad (21)$$

Using the identities $\mathrm{d}(a/b) = (b\mathrm{d}a - a\mathrm{d}b)/b^2$ and $\mathrm{d}(a \cdot b) = \mathrm{d}a \cdot b + a \cdot \mathrm{d}b$,

$$\mathrm{d}(\cos\theta) = \frac{\mathbf{m}_2 \cdot \mathrm{d}\mathbf{s}_2}{[1 - (\mathbf{m}_2\cdot\mathbf{k})(\mathbf{s}_2\cdot\mathbf{k})]} - \frac{(1 - \mathbf{m}_2\cdot\mathbf{s}_2)(\mathbf{m}_2\cdot\mathbf{k})(\mathrm{d}\mathbf{s}_2\cdot\mathbf{k})}{[1 - (\mathbf{m}_2\cdot\mathbf{k})(\mathbf{s}_2\cdot\mathbf{k})]^2} \quad (22)$$

$$|\mathrm{d}(\cos\theta)| = \left|\frac{\mathbf{m}_2 \cdot \mathrm{d}\mathbf{s}_2}{\sin^2\theta_m} + \frac{(1-\cos\theta)\mathrm{d}\theta_m}{\tan\theta_m}\right|. \quad (23)$$

Since $\mathrm{d}(\cos\theta) = \sin\theta\mathrm{d}\theta$

$$|\mathrm{d}\theta| = \left|\frac{\mathbf{m}_2 \cdot \mathrm{d}\mathbf{s}_2}{\sin\theta\sin^2\theta_m} + \frac{(1-\cos\theta)\mathrm{d}\theta_m}{\sin\theta\tan\theta_m}\right|. \quad (24)$$

Using Schwartz's inequality we get an upper bound on the value of the error as

$$|\mathrm{d}(\cos\theta)| \leq \left|\frac{\mathbf{m}_2 \cdot \mathrm{d}\mathbf{s}_2}{\sin^2\theta_m}\right| + \left|\frac{(1-\cos\theta)\mathrm{d}\theta_m}{\tan\theta_m}\right| \quad (25)$$

$$|\mathrm{d}\theta| \leq \left|\frac{\mathbf{m}_2 \cdot \mathrm{d}\mathbf{s}_2}{\sin\theta\sin^2\theta_m}\right| + \left|\frac{(1-\cos\theta)\mathrm{d}\theta_m}{\sin\theta\tan\theta_m}\right|. \quad (26)$$

Since $|\mathbf{m}_2 \cdot \mathrm{d}\mathbf{s}_2| = |\mathbf{m}_2|\,|\mathrm{d}\mathbf{s}_2| \cos\beta \le \mathrm{d}\theta_m$ where β is the angle between $\mathrm{d}\mathbf{s}_2$ and $\mathbf{m}_2$,

$$|\mathrm{d}(\cos\theta)| \le \frac{\mathrm{d}\theta_m}{\sin^2\theta_m} + |(1-\cos\theta)| \frac{1}{|\tan\theta_m|}\mathrm{d}\theta_m \tag{27}$$

$$|\mathrm{d}\theta| \le \frac{\mathrm{d}\theta_m}{|\sin\theta|\sin^2\theta_m} + \left|\frac{(1-\cos\theta)}{\sin\theta}\right| \frac{1}{|\tan\theta_m|}\mathrm{d}\theta_M. \tag{28}$$

The asymptotic behavior of $|\mathrm{d}\theta|$ and $|\mathrm{d}(\cos\theta)|$ with respect to θ_m and θ is as follows:

As $\theta \to 0$, $|\mathrm{d}\theta| \to \infty$, $|\mathrm{d}(\cos\theta)| \to \dfrac{\mathrm{d}\theta_m}{\sin^2\theta_m}$

As $\theta \to \dfrac{\pi}{2}$, $|\mathrm{d}\theta| \to \mathrm{d}\theta_m \left(\dfrac{1}{\sin^2\theta_m} + \dfrac{1}{|\tan\theta_m|}\right)$,

$|\mathrm{d}(\cos\theta)| \to \mathrm{d}\theta_m \left(\dfrac{1}{\sin^2\theta_m} + \dfrac{1}{|\tan\theta_M|}\right)$

As $\theta \to \pi$, $|\mathrm{d}\theta| \to \infty$,

$|\mathrm{d}(\cos\theta)| \to \mathrm{d}\theta_m \left(\dfrac{1}{\sin^2\theta_m} + \dfrac{2}{|\tan\theta_m|}\right)$

As $\theta_m \to 0$, $|\mathrm{d}\theta| \to \infty$, $|\mathrm{d}(\cos\theta_m)| \to \infty$

As $\theta_m \to \dfrac{\pi}{2}$, $|\mathrm{d}\theta| \to \dfrac{\mathrm{d}\theta_M}{|\sin\theta|}$, $|\mathrm{d}(\cos\theta)| \to \mathrm{d}\theta_m$

As $\theta_m \to \pi$, $|\mathrm{d}\theta| \to \infty$, $|\mathrm{d}(\cos\theta)| \to \infty$.

For a given value of $\mathrm{d}\theta_m$ we have an error surface $\varepsilon = \varepsilon(\theta, \theta_m)$.

Case 2.

$$\mathbf{m}_2 = \mathbf{s}_2 \Rightarrow \mathbf{k} = \mathbf{s}_2 = \mathbf{m}_2 \tag{29}$$

thus

$$\mathrm{d}\mathbf{k} = \mathrm{d}\mathbf{s}_2, \tag{30}$$

$$\mathbf{m}_1 \cdot \mathbf{m}_2 = \mathbf{m}_1 \cdot \mathbf{k} = \cos\theta_m$$

$$\text{and } \mathbf{s}_1 \cdot \mathbf{s}_2 = \mathbf{s}_1 \cdot \mathbf{k} = \cos\theta_m \tag{31}$$

since

$$\cos\theta = 1 - \frac{[1-(\mathbf{m}_1 \cdot \mathbf{s}_1)]}{[1-(\mathbf{k}\cdot\mathbf{m}_1)(\mathbf{k}\cdot\mathbf{s}_1)]} \tag{32}$$

$$\mathrm{d}(\cos\theta) = -\mathrm{d}\left[\frac{1-(\mathbf{m}_1\cdot\mathbf{s}_1)}{1-(\mathbf{k}\cdot\mathbf{m}_1)(\mathbf{k}\cdot\mathbf{s}_1)}\right]. \tag{33}$$

Using the results in (30) and (31)

$$|\mathrm{d}(\cos\theta)| = |(1-\cos\theta)| \left|\frac{|\cos\theta_m|}{\sin^2\theta_m}\right| |\mathbf{m}_1\cdot\mathrm{d}\mathbf{s}_2 + \mathbf{s}_1\cdot\mathrm{d}\mathbf{s}_2| \tag{34}$$

$$|\mathrm{d}\theta| = \left|\frac{(1-\cos\theta)}{\sin\theta}\right| \left|\frac{|\cos\theta_m|}{\sin^2\theta_m}\right| |\mathbf{m}_1\cdot\mathrm{d}\mathbf{s}_2 + \mathbf{s}_1\cdot\mathrm{d}\mathbf{s}_2|. \tag{35}$$

Using Schwartz's inequality

$$|\mathrm{d}(\cos\theta)| \le |(1-\cos\theta)| \frac{|\cos\theta_m|}{\sin^2\theta_m}(|\mathbf{m}_1\cdot\mathrm{d}\mathbf{s}_2| + |\mathbf{s}_1\cdot\mathrm{d}\mathbf{s}_2|) \tag{36}$$

$$|\mathrm{d}\theta| \le \left|\frac{(1-\cos\theta)}{\sin\theta}\right| \frac{|\cos\theta_m|}{\sin^2\theta_m}(|\mathbf{m}_1\cdot\mathrm{d}\mathbf{s}_2| + |\mathbf{s}_1\cdot\mathrm{d}\mathbf{s}_2|). \tag{37}$$

Since

$$|\mathbf{m}_1\cdot\mathrm{d}\mathbf{s}_2| = |\mathbf{m}_1|\,|\mathrm{d}\mathbf{s}_2|\cos\gamma \le \mathrm{d}\theta_m$$

where γ is the angle between $\mathbf{m}_1$ and $\mathrm{d}\mathbf{s}_2$ and

$$|\mathbf{s}_1\cdot\mathrm{d}\mathbf{s}_2| = |\mathbf{s}_1|\,|\mathrm{d}\mathbf{s}_2|\cos\alpha \le \mathrm{d}\theta_m,$$

where α is the angle between $\mathbf{s}_1$ and $\mathrm{d}\mathbf{s}_2$ and

$$|\mathrm{d}(\cos\theta)| \le 2|(1-\cos\theta)| \frac{|\cos\theta_m|}{\sin^2\theta_m}\mathrm{d}\theta_m \tag{38}$$

$$|\mathrm{d}\theta| \le \left|\frac{2(1-\cos\theta)}{\sin\theta}\right| \frac{|\cos\theta_m|}{\sin^2\theta_m}\mathrm{d}\theta_m. \tag{39}$$

The asymptotic behaviour of $|\mathrm{d}\theta|$ and $|\mathrm{d}(\cos\theta)|$ with respect to θ_m and θ is as follows:

As $\theta \to 0$, $|\mathrm{d}\theta| \to 0$, $|\mathrm{d}(\cos\theta)| \to 0$

As $\theta \to \dfrac{\pi}{2}$, $|\mathrm{d}\theta| \to \dfrac{2|\cos\theta_m|}{\sin^2\theta_m}\mathrm{d}\theta_m$,

$|\mathrm{d}(\cos\theta)| \to \dfrac{2|\cos\theta_m|}{\sin^2\theta_m}\mathrm{d}\theta_m$

As $\theta \to \pi$, $|\mathrm{d}\theta| \to \infty$, $|\mathrm{d}(\cos\theta)| \to \dfrac{4|\cos\theta_m|}{\sin^2\theta_m}\mathrm{d}\theta_m$

As $\theta_m \to \theta$, $|\mathrm{d}\theta| \to \infty$, $|\mathrm{d}(\cos\theta_m)| \to \infty$

As $\theta_m \to \dfrac{\pi}{2}$ $|\mathrm{d}\theta| \to 0$, $|\mathrm{d}(\cos\theta| \to 0$

As $\theta_m \to \pi$, $|\mathrm{d}\theta| \to \infty$, $|\mathrm{d}(\cos\theta)| \to \infty$.

Case 3.

$$\mathbf{m}_1 \ne \mathbf{k} \ne \mathbf{s}_1 \text{ and } \mathbf{m}_2 \ne \mathbf{k} \ne \mathbf{s}_2.$$

From (4),

$$\mathbf{k} = \frac{(\mathbf{m}_1-\mathbf{s}_1)\otimes(\mathbf{m}_2-\mathbf{s}_2)}{|(\mathbf{m}_1-\mathbf{s}_1)\otimes(\mathbf{m}_2-\mathbf{s}_2)|} = \frac{(\mathbf{m}_1-\mathbf{s}_1)\otimes(\mathbf{m}_2-\mathbf{s}_2)}{M} \tag{40}$$

where

$$M \triangleq |(\mathbf{m}_1-\mathbf{s}_1)\otimes(\mathbf{m}_2-\mathbf{s}_2)| = [((\mathbf{m}_1-\mathbf{s}_1)\otimes(\mathbf{m}_2-\mathbf{s}_2))\cdot((\mathbf{m}_1-\mathbf{s}_1)\otimes(\mathbf{m}_2-\mathbf{s}_2))]^{\frac{1}{2}} \tag{41}$$

$$\mathrm{d}\mathbf{k} = \mathrm{d}\left[\frac{(\mathbf{m}_1-\mathbf{s}_1)\otimes(\mathbf{m}_2-\mathbf{s}_2)}{|\mathbf{m}_1-\mathbf{s}_1)\otimes(\mathbf{m}_2-\mathbf{s}_2)|}\right] \tag{42}$$

$$\mathbf{dk} = (M\mathrm{d}[(\mathbf{m}_1 - \mathbf{s}_1) \otimes (\mathbf{m}_2 - \mathbf{s}_2)] - [(\mathbf{m}_1 - \mathbf{s}_1) \otimes (\mathbf{m}_2 - \mathbf{s}_2)]\,\mathrm{d}M)/M^2. \tag{43}$$

On simplification this yields

$$\mathbf{dk} = \frac{1}{M}[\mathbf{ds}_2 \otimes (\mathbf{m}_1 - \mathbf{s}_2)] - \frac{1}{M}\mathbf{k}[\mathbf{k} \cdot [\mathbf{ds}_2 \otimes (\mathbf{m}_1 - \mathbf{s}_1)]]. \tag{44}$$

Since $\mathbf{k} \cdot \mathbf{k} = 1$,

$$\mathbf{k} \cdot \mathbf{dk} = 0. \tag{45}$$

From (44) and (45),

$$\mathbf{dk} = \frac{1}{M}[\mathbf{ds}_2 \otimes (\mathbf{m}_1 - \mathbf{s}_1)] \tag{46}$$

$$|\mathbf{dk}| = \frac{1}{M}|\mathbf{ds}_2|\,|\mathbf{m}_1 - \mathbf{s}_1| \sin \beta \tag{47}$$

$$|\mathbf{dk}| = \frac{1}{M}\mathrm{d}\theta_m |\mathbf{m}_1 - \mathbf{s}_1| \sin \beta \tag{48}$$

where β is the angle between $\mathbf{ds}_2$ and $\mathbf{m}_1 - \mathbf{s}_1$

$$|\mathbf{dk}| \le \frac{1}{M}\mathrm{d}\theta_m. \tag{49}$$

Thus $\mathbf{dk}$ is directly proportional to $\mathrm{d}\theta_m$ and inversely proportional to M.

Case 3.1.

$$\cos\theta = 1 - \frac{[1 - (\mathbf{m}_1 \cdot \mathbf{s}_1)]}{[1 - (\mathbf{k} \cdot \mathbf{m}_1)(\mathbf{k} \cdot \mathbf{s}_1)]}. \tag{50}$$

Thus,

$$\mathrm{d}(\cos\theta) = -\mathrm{d}\left[\frac{1 - (\mathbf{m}_1 \cdot \mathbf{s}_1)}{1 - (\mathbf{k} \cdot \mathbf{m}_1)(\mathbf{k} \cdot \mathbf{s}_1)}\right] \tag{51}$$

$$= \frac{(1 - \mathbf{m}_1 \cdot \mathbf{s}_1)\mathrm{d}[1 - (\mathbf{m}_1 \cdot \mathbf{k})(\mathbf{s}_1 \cdot \mathbf{k})]}{[1 - (\mathbf{m}_1 \cdot \mathbf{k})(\mathbf{s}_1 \cdot \mathbf{k})]^2}. \tag{52}$$

Since $\mathbf{m}_1 \cdot \mathbf{k} = \mathbf{s}_1 \cdot \mathbf{k}$

$$\mathrm{d}(\cos\theta) = \frac{(1 - \mathbf{m}_1 \cdot \mathbf{s}_1)\mathrm{d}[1 - (\mathbf{m}_1 \cdot \mathbf{k})^2]}{[1 - (\mathbf{m}_1 \cdot \mathbf{k})^2]^2} \tag{53}$$

$$= \frac{-2(1 - \mathbf{m}_1 \cdot \mathbf{s}_1)(\mathbf{m}_1 \cdot \mathbf{k})(\mathbf{m}_1 \cdot \mathbf{dk})}{[1 - (\mathbf{m}_1 \cdot \mathbf{k})^2]^2} \tag{54}$$

$$= \frac{-2(1 - \mathbf{m}_1 \cdot \mathbf{s}_1)(\mathbf{m}_1 \cdot \mathbf{k})(\mathbf{m}_1 \cdot \mathbf{dk})}{[1 + (\mathbf{m}_1 \cdot \mathbf{k})]^2[1 - (\mathbf{m}_1 \cdot \mathbf{k})]^2}. \tag{55}$$

From (46),

$$\mathbf{m}_1 \cdot \mathbf{dk} = \frac{\mathbf{m}_1}{M} \cdot [\mathbf{ds}_2 \otimes (\mathbf{m}_1 - \mathbf{s}_1)]. \tag{56}$$

Using the trigonometric identity $\mathbf{A} \cdot (\mathbf{B} \otimes \mathbf{C}) = (\mathbf{A} \otimes \mathbf{B}) \cdot \mathbf{C} = (\mathbf{C} \otimes \mathbf{A}) \cdot \mathbf{B}$ and with $\cos\lambda \triangleq \mathbf{m}_1 \cdot \mathbf{k}$,

$$\mathbf{m}_1 \cdot \mathbf{dk} = \frac{\mathbf{ds}_2}{M} \cdot [(\mathbf{m}_1 - \mathbf{s}_1) \otimes \mathbf{m}_1] \tag{57}$$

$$\mathbf{m}_1 \cdot \mathbf{dk} = \frac{\mathbf{ds}_2}{M} \cdot [\mathbf{m}_1 \otimes \mathbf{s}_1] \tag{58}$$

$$|\mathbf{m}_1 \cdot \mathbf{dk}| = \frac{|\mathbf{ds}_2|\,|\mathbf{m}_1 \otimes \mathbf{s}_1| \cos\beta}{M} \le \frac{\mathrm{d}\theta_m}{M} \tag{59}$$

where β is the angle between $\mathbf{ds}_2$ and $\mathbf{m}_1 \otimes \mathbf{s}_1$

$$|\mathrm{d}(\cos\theta)| = 2|(1 - \cos\theta)|\frac{|\cos\lambda|}{\sin^2\lambda}|\mathbf{m}_1 \cdot \mathbf{dk}|. \tag{60}$$

From (59) and (60)

$$|\mathrm{d}(\cos\theta)| \le \frac{2|(1 - \cos\theta)|\,|\cos\lambda|}{M \sin^2\lambda}\mathrm{d}\theta_m. \tag{61}$$

Since $\mathrm{d}(\cos\theta) = -\sin\theta \mathrm{d}\theta$, (60) yields

$$|\mathrm{d}\theta| = \left|\frac{2(1 - \cos\theta)}{\sin\theta}\right| \frac{|\cos\lambda|}{\sin^2\lambda}|\mathbf{m}_1 \cdot \mathbf{dk}|. \tag{62}$$

From (59) and (62) we get

$$|\mathrm{d}\theta| \le \left|\frac{2(1 - \cos\theta)}{M\sin\theta}\right| \frac{|\cos\lambda|}{\sin^2\lambda}\mathrm{d}\theta_m. \tag{63}$$

The asymptotic analysis for $|\mathrm{d}\theta|$ and $|\mathrm{d}(\cos\theta)|$ is as follows:

As $\theta \to 0$, $|\mathrm{d}\theta| \to 0$, $|\mathrm{d}(\cos\theta)| \to 0$

As $\theta \to \frac{\pi}{2}$, $|\mathrm{d}\theta| \to \frac{2}{M}\frac{|\cos\lambda|}{\sin^2\lambda}\mathrm{d}\theta_m$,

$|\mathrm{d}(\cos\theta)| \to \frac{2}{M}\frac{|\cos\lambda|}{\sin^2\lambda}\mathrm{d}\theta_m$

As $\theta \to \pi$, $|\mathrm{d}\theta| \to \infty$, $|\mathrm{d}(\cos\theta)| \to \frac{4}{M}\frac{|\cos\lambda|}{M\sin^2\lambda}\mathrm{d}\theta_m$

As $\lambda \to 0$, $|\mathrm{d}\theta| \to \infty$, $|\mathrm{d}(\cos\theta)| \to \infty$

As $\lambda \to \frac{\pi}{2}$, $|\mathrm{d}\theta| \to 0$, $|\mathrm{d}(\cos\theta)| \to 0$

As $\lambda \to \pi$, $|\mathrm{d}\theta| \to \infty$, $|\mathrm{d}(\cos\theta)| \to \infty$.

Case 3.2.

$$\cos\theta = 1 - \frac{[1 - (\mathbf{m}_2 \cdot \mathbf{s}_2)]}{[1 - (\mathbf{k} \cdot \mathbf{m}_2)(\mathbf{k} \cdot \mathbf{s}_2)]}. \tag{64}$$

Thus,

$$\mathrm{d}(\cos\theta) = -\mathrm{d}\left[\frac{1 - (\mathbf{m}_2 \cdot \mathbf{s}_2)}{1 - (\mathbf{k} \cdot \mathbf{m}_2)(\mathbf{k} \cdot \mathbf{s}_2)}\right]. \tag{65}$$

Since $\mathbf{m}_2 \cdot \mathbf{k} = \mathbf{s}_2 \cdot \mathbf{k}$,

$$\mathrm{d}(\cos\theta) = -\mathrm{d}\left[\frac{1 - (\mathbf{m}_2 \cdot \mathbf{s}_2)}{1 - (\mathbf{k} \cdot \mathbf{m}_2)^2}\right] = \frac{\mathbf{m}_2 \cdot \mathbf{ds}_2}{[1 - (\mathbf{m}_2 \cdot \mathbf{k})^2]} - \frac{(1 - \mathbf{m}_2 \cdot \mathbf{s}_2)2(\mathbf{m}_2 \cdot \mathbf{k})(\mathbf{m}_2 \cdot \mathbf{dk})}{[1 - (\mathbf{m}_2 \cdot \mathbf{k})^2]^2} \tag{66}$$

$$|\mathrm{d}(\cos\theta)| = \left|\frac{\mathbf{m}_2 \cdot \mathbf{ds}_2}{[1 - (\mathbf{m}_2 \cdot \mathbf{k})^2]} + \frac{(1 - \mathbf{m}_2 \cdot \mathbf{s}_2)(-2)(\mathbf{m}_2 \cdot \mathbf{k})(\mathbf{m}_2 \cdot \mathbf{dk})}{[1 - (\mathbf{m}_2 \cdot \mathbf{k})^2]^2}\right|. \tag{67}$$

Using Schwartz's inequality

$$|\mathrm{d}(\cos\theta)| \le \left|\frac{\mathbf{m}_2\cdot \mathrm{d}\mathbf{s}_2}{[1-(\mathbf{m}_2\cdot\mathbf{k})^2]}\right| + \left|\frac{(1-\mathbf{m}_2\cdot\mathbf{s}_2)(-2)(\mathbf{m}_2\cdot\mathbf{k})(\mathbf{m}_2\cdot\mathrm{d}\mathbf{k})}{[1-(\mathbf{m}_2\cdot\mathbf{k})^2]^2}\right|. \quad (68)$$

From (46),

$$\mathbf{m}_2\cdot\mathrm{d}\mathbf{k} = \frac{\mathbf{m}_2}{M}\cdot[\mathrm{d}\mathbf{s}_2\otimes(\mathbf{m}_1-\mathbf{s}_1)]. \quad (69)$$

Using the trigonometric identity $\mathbf{A}\cdot(\mathbf{B}\otimes C) = (\mathbf{A}\otimes\mathbf{B})\cdot\mathbf{C} = (\mathbf{C}\otimes\mathbf{A})\cdot\mathbf{B}$ and with $\cos\lambda \triangleq \mathbf{m}_2\cdot\mathbf{k}$,

$$\mathbf{m}_2\cdot\mathrm{d}\mathbf{k} = \frac{\mathrm{d}\mathbf{s}_2}{M}\cdot[(\mathbf{m}_1-\mathbf{s}_1)\otimes\mathbf{m}_2]$$

$$= \frac{|\mathrm{d}\mathbf{s}_2|}{M}|[(\mathbf{m}_1-\mathbf{s}_1)\otimes\mathbf{m}_2]|\cos\beta \quad (70)$$

$$\le \frac{|\mathrm{d}\mathbf{s}_2|}{M} = \frac{\mathrm{d}\theta_m}{M} \quad (71)$$

$$\mathbf{m}_2\cdot\mathrm{d}\mathbf{s}_2 = |\mathrm{d}\mathbf{s}_2|\,|\mathbf{m}_2|\cos\alpha \le |\mathrm{d}\mathbf{s}_2| = \mathrm{d}\theta_m \quad (72)$$

where α is the angle between $\mathrm{d}\mathbf{s}_2$ and $\mathbf{m}_2$, (68)–(73) yield

$$|\mathrm{d}(\cos\theta)| \le \frac{\mathrm{d}\theta_m}{\sin^2\lambda} + \left|\frac{2(1-\cos\theta)}{M}\right|\frac{|\cos\lambda|}{\sin^2\lambda}\mathrm{d}\theta_m. \quad (73)$$

Using the fact that $|\mathrm{d}(\cos\theta)| = |\sin\theta \mathrm{d}\theta|$

$$|\mathrm{d}\theta| \le \frac{\mathrm{d}\theta_m}{|\sin\theta|\sin^2\lambda} + \left|\frac{2(1-\cos\theta)}{M\sin\theta}\right|\frac{|\cos\lambda|}{\sin^2\lambda}\mathrm{d}\theta_m. \quad (74)$$

The asymptotic analysis for $|\mathrm{d}\theta|$ and $|\mathrm{d}(\cos\theta)|$ is as follows:

As $\lambda\to 0$, $|\mathrm{d}\theta|\to\infty$, $|\mathrm{d}(\cos\theta)|\to\infty$

As $\lambda\to\frac{\pi}{2}$, $|\mathrm{d}\theta|\to\frac{\mathrm{d}\theta_m}{|\sin\theta|}$, $|\mathrm{d}(\cos\theta)|\to\mathrm{d}\theta_m$

As $\lambda\to\pi$, $|\mathrm{d}\theta|\to\infty$, $|\mathrm{d}(\cos\theta)|\to\infty$

As $\theta\to 0$, $|\mathrm{d}\theta|\to\infty$, $|\mathrm{d}(\cos\theta)|\to\frac{\mathrm{d}\theta_m}{\sin^2\lambda}$

As $\theta\to\frac{\pi}{2}$, $|\mathrm{d}\theta|\to\frac{\mathrm{d}\theta_m}{\sin^2\lambda}+\frac{2}{M}\frac{|\cos\lambda|}{M\sin^2\lambda}\mathrm{d}\theta_m$

$$|\mathrm{d}(\cos\theta)|\to\frac{\mathrm{d}\theta_m}{\sin^2\lambda}+\frac{2|\cos\lambda|}{M\sin^2\lambda}\mathrm{d}\theta_m$$

As $\theta\to|\mathrm{d}\theta|\to\infty$, $|\mathrm{d}(\cos\theta)|\to\frac{\mathrm{d}\theta_m}{\sin^2\lambda}+\frac{4}{M}\frac{|\cos\lambda|}{\sin^2\lambda}\mathrm{d}\theta_m$.

In all the above three cases it can be seen that the error in $|\theta|$ is higher than the error in $|\cos\theta|$,

of course, since $|\mathrm{d}\theta| = \frac{|\mathrm{d}\cos\theta|}{|\sin\theta|}$ and $0 < |\sin\theta| < 1$.

Since the axis of rotation $k = [k_x,\ k_y,\ k_z] = [\cos\xi\sin\eta,\ \sin\xi\sin\eta,\ \cos\eta]$

$$\mathrm{d}k_x = -\sin\xi\sin\eta\,\mathrm{d}\xi + \cos\xi\cos\eta\,\mathrm{d}\eta \quad (75)$$

$$\mathrm{d}k_y = \cos\xi\sin\eta\,\mathrm{d}\xi + \sin\xi\cos\eta\,\mathrm{d}\eta \quad (76)$$

$$\mathrm{d}k_z = -\sin\eta\,\mathrm{d}\eta. \quad (77)$$

(76) and (77) yield

$$\mathrm{d}\xi = \frac{1}{\sin\eta}(\sin\xi\mathrm{d}k_x - \cos\xi\mathrm{d}k_y) \quad (78)$$

$$\mathrm{d}\eta = \frac{1}{\cos\eta}(\cos\xi\mathrm{d}k_x + \sin\xi\mathrm{d}k_y). \quad (79)$$

Thus, as $\eta\to 0$ or π, $\mathrm{d}\xi\to\infty$ and as $\eta\to(\pi/2)$, $\mathrm{d}\eta\to\infty$. Assuming that the errors $\mathrm{d}k_y$ and $\mathrm{d}k_z$ are of the same order as $|\mathbf{dk}|$, the errors in ξ and η are greater than $|\mathbf{dk}|$. From (15) and assuming that there is no error in the model coordinates x_0, y_0 and z_0,

$$\mathrm{d}t_x = \mathrm{d}u_0 - \mathrm{d}r_{11}x_0 - \mathrm{d}r_{12}y_0 - \mathrm{d}r_{13}z_0$$

$$\mathrm{d}t_y = \mathrm{d}v_0 - \mathrm{d}r_{21}x_0 - \mathrm{d}r_{22}y_0 - \mathrm{d}r_{23}z_0$$

$$\mathrm{d}t_z = \mathrm{d}w_0 - \mathrm{d}r_{31}x_0 - \mathrm{d}r_{32}y_0 - \mathrm{d}r_{33}z_0. \quad (80)$$

From (81) and the expressions for r_{11}, r_{12}, r_{13}, r_{21}, r_{22}, r_{23}, r_{31}, r_{32} and r_{33} in (14),

$$(\mathrm{d}t_x)_{\max} \approx \max[\mathrm{d}u_0, \mathrm{d}(\cos\theta), \mathrm{d}(\sin\theta), \mathrm{d}k_x, \mathrm{d}k_y, \mathrm{d}k_z] \quad (81)$$

$$(\mathrm{d}t_y)_{\max} \approx \max[\mathrm{d}v_0, \mathrm{d}(\cos\theta), \mathrm{d}(\sin\theta), \mathrm{d}k_x, \mathrm{d}k_y, \mathrm{d}k_z] \quad (82)$$

$$(\mathrm{d}t_z)_{\max} \approx \max[\mathrm{d}w_0, \mathrm{d}(\cos\theta), \mathrm{d}(\sin\theta), \mathrm{d}k_x, \mathrm{d}k_y, \mathrm{d}k_z]. \quad (83)$$

$\mathrm{d}(\sin\theta)$ is of the same order of magnitude as $\mathrm{d}(\cos\theta)$ if $\mathrm{d}(\sin\theta)\approx 10.0\mathrm{d}(\cos\theta)$, which implies that $5.71\le\theta\le 174.29$ which is very often the case. From Equations (76)–(78) and (82)–(84) it can be seen that the estimates of the rotation parameters ξ, η and θ are more sensitive than the translation parameters t_x, t_y, and t_z (assuming that the error in (u_0, v_0, w_0) is small, which seems reasonable).

A straightforward way of making the computed pose more robust to the difference in the angle between the model and scene dihedral junctions or dihedral feature junctions is by introducing redundancy in the parameter space. For example the axis of rotation $\mathbf{k}$ could be presented by the triple (k_x, k_y, k_z) rather than the double (ξ, η) since parameters k_x, k_y and k_z are more robust than the parameters ξ and η. Similarly, the angle of rotation θ can be replaced by the double ($\cos\theta$, $\sin\theta$) which uniquely specifies the angle θ in the range $-\pi\le\theta\le\pi$. Since the values of $\sin\theta$ and $\cos\theta$ are less sensitive than the value of θ, replacing θ by the double ($\cos\theta$, sin θ) would ensure greater robustness in the computed pose.

4. CONCLUSIONS

In this paper we have formally analysed the sensitivity of the computed pose parameters to the difference in the angles of the scene and the model dihedral junctions. We have shown how the rotation parameters ξ, η and θ are more sensitive to the difference in the included angles of the scene and model dihedral junctions or dihedral feature junctions as compared to the translation parameters t_x, t_y and t_z. We have also shown how the pose computation could be made more robust at the cost of adding redundancy in the parameter space. The formal analysis presented in this paper is supported by the experiments in our previous work.[4,5]

SUMMARY

Recognition-via-localization is a popular paradigm in model-based vision. Primitive geometric features are extracted from the scene. These features are matched against similar features in the model. The matches are constrained by length and angle measurements. The constraints that arise from the matching of these features are propagated using a constraint propagation/constraint satisfaction technique. A consistent set of constraints constitutes a valid scene interpretation. In this sense, a scene interpretation problem could be looked upon as a constraint propagation/constraint satisfaction problem.

Hough clustering is a popular constraint propagation/constraint satisfaction technique owing to its conceptual simplicity and potential ease of parallelization. Each match of a scene feature with a model feature is used to compute a geometric transformation that places the model feature in registration with the scene feature. The geometric transformation is characterized by a feature vector. The dimensionality of the feature vector is determined by the number of degrees of freedom that the objects in the scene possess. For three-dimensional object recognition with six degrees of freedom, the feature vector is a six-tuple. Each match of a scene feature to a model feature can thus be represented as a point in six-dimensional parameter (Hough) space. Clustering of points in the Hough space is used to determine the global pose of the object.

In our previous work we had shown the advantages of using dihedral junctions as features for recognition and localization of polyhedral objects. These were further generalized to dihedral feature junctions for the recognition and localization of complex objects made up of piecewise combinations of conical, cylindrical, spherical and planar surfaces. In our experimental results we observed that the rotational parameters of the computed pose were more sensitive than the translational parameters to the difference in the included angle of the scene and the model dihedral junction. In this paper we have carried out a formal sensitivity analysis where the sensitivity of the computed pose to the difference in the included angle of the scene and the model dihedral junction is analytically computed. The work in this paper could be thus treated as a sequel to our previous work. The results of the sensitivity analysis were found to be in conformity with the experimental results from our previous work. It has been shown how the introduction of redundancy in the Hough pose results in greater robustness in the computed pose. Although the sensitivity analysis in this paper is based on matching and pose computation using dihedral junctions and dihedral feature junctions, the analysis technique is general enough to be extended to matching and pose computation using other feature types.

REFERENCES

1. G. Stockman, Object recognition and localization via post clustering, *Comput. Vision Graphics Image Process.* **40**, 361–387 (1987).
2. B. A. Boyter and J. K. Aggarwal, Recognition of polyhedra from range data, *IEEE Expert*, pp. 47–59 (1986).
3. M. Dhome and T. Kasavand, Polyhedra recognition by hypothesis accumulation *IEEE Trans. Pattern Anal. Mach. Intell.* **9**, 429–438 (1987).
4. S. M. Bhandarkar and Minsoo Suk, Hough clustering technique for surface matching, *Proc. IAPR Wkshop Comput. Vision*, Tokyo, Japan, pp. 82–85.
5. S. M. Bhandarkar and Minsoo Suk, Recognition and localization of objects with curved surfaces, *Mach. Vision Appl.* (in press).
6. W. E. L. Grimson and T. Lozano-Perez, Localizing overlapping parts by searching the interpolation tree, *IEEE Trans. Pattern Anal. Mach. Intell.* **9**, 469–482 (1987).
7. T. Nagata and H. B. Zha, Determining orientation, location and size of primitive surfaces by a modified Hough transformation technique, *Pattern Recognition* **21**, 481–491 (1988).
8. R. P. Paul, *Robot Manipulators: Mathematics, Programming and Control.* MIT Press, Cambridge, MA (1981).
9. G. A. Korn and T. M. Korn, *Mathematical Handbook for Scientists and Engineers.* McGraw-Hill, New York (1972).

About the Author—S. M. BHANDARKAR received his B.Tech. in Electrical Engineering from the Indian Institute of Technology, Bombay, India, in 1983, and his M.S. and Ph.D. in Computer Engineering from Syracuse University, Syracuse, New York, in 1985 and 1989, respectively. He is currently an Assistant Professor in the Department of Computer Science at the University of Georgia in Athens. He was nominated University Fellow for the academic years 1986–87 and 1987–88. He is a member of IEEE, AAAI and Phi Kappa Phi. His research interests include computer vision, pattern recognition, image processing and artificial intelligence.

About the Author—MINSOO SUK received his B.S., M.S. and Ph.D. degrees, all in Electrical Engineering in 1970, 1972 and 1974, respectively, from the University of California at Davis. He is currently an Associate Professor in the Department of Electrical and Computer Engineering at Syracuse University, Syracuse, New York. Before joining Syracuse University, he was a member of Technical Staff at Rockwell International, and an Associate Professor at the Korea Advanced Institute of Science and Technology. His research interests include computer vision, pattern recognition, image processing, computational geometry, artificial intelligence, knowledge-based systems and parallel architectures and algorithms.